Click-Chemistry Approach towards Antibacterial and Degradable

Hybrid Hydrogels Based on Octa-Betaine Ester Polyhedral

Oligomeric Silsesquioxane

Jin Han¹, Qinyue Chen¹, Yupeng Shen¹, Zhixiong Liu^{2*}, Xiaoyu Hao², Mingqiang Zhong¹, Michael R. Bockstaller³*

Department of Materials Science & Engineering, Zhejiang University of Technology,

Hangzhou, 310014, P. R. China

2) School of Chemistry and Environmental Engineering, Shanxi Datong University, Datong,

037009, P. R. China

3) Department of Materials Science & Engineering, Carnegie Mellon University, 5000 Forbes

Ave., Pittsburgh, PA 15213, United States

Correspondence to:

liuzhixiong@iccas.ac.cn

bockstaller@cmu.edu

1

ABSTRACT

An efficient process for the synthesis of degradable hydrogels containing octa-betaine ester

polyhedral oligomeric silsesquioxane (POSS) through efficient thiol-ene and Menschutkin

click reactions was developed. The hydrogels exhibited a yield strength of 0.36 MPa and a

compressive modulus of 4.38 MPa and displayed excellent flexibility as well as torsion

resistance. Antibacterial efficacy of hydrogels (and degradation products) was evaluated using

Escherichia coli (Gram-negative) and Staphylococcus aureus (Gram-positive). Efficacy was

found to increase with the concentration of cetyl chloroacetate (CCA) in the hydrogel network,

reaching 93% and 99% for Escherichia coli and Staphylococcus aureus, respectively.

Degradation of hydrogels was observed in weak alkali conditions (pH = 8) and at physiological

conditions (pH = 7.4). The degradation time of the hydrogels could be finely tuned by variation

of the CCA content in the hydrogel and environmental stimulus. The tunable degradation

behavior under physiological conditions combined with high antibacterial efficacy could

render the presented materials interesting for tissue engineering applications.

Keywords: Hybrid Hydrogel; Click-Chemistry; Degradable; POSS; Antibacterial

2

INTRODUCTION

Hydrogel materials are 3D porous polymer networks with high water content and tissue-like softness. This has rendered them candidate materials in applications such as tissue engineering, biosensing and drug delivery.¹⁻³ Important features of hydrogels include biocompatibility, biodegradability and antibacterial behavior. Biocompatibility is a prerequisite for therapeutic applications. Biocompatibility has been reported for hydrogels composed of poly(ethylene glycol) (PEG)⁴, polysaccharides⁵ or other hydrophilic polymers⁶. Tunable degradation behavior under physiological conditions is a desirable attribute for hydrogels used in tissue engineering applications as the degradation process can provide space to promote cell proliferation and infiltration of blood vessels.⁷ Antimicrobial behavior is important because it can reduce inflammation processes during regenerative medical procedures.⁸⁻⁹ One example are quarternary ammonium salts (QAS) that have been used to realize hydrogels with broad antimicrobial activity against bacteria, fungi and viruses^{5, 10}. However, a key problem with QAS hydrogels is 'fouling' that occurs by deposition of the dead microorganisms on the hydrogel surface. Fouling reduces the effectiveness of antimicrobial moieties and thus is a frequent cause of inflammatory processes. The modification of surfaces with zwitterionic groups (for example, based on hydrolyzed betaine esters) has shown to be effective to avoid 'fouling' and thus prolong the antibacterial function of surfaces. 11-12 The integration of QAS groups into hydrogel networks through cleavable bonds is therefore considered to be a promising strategy to develop biodegradable and antibacterial soft materials.

Various coupling methodologies based on covalent chemical cross-linking and physical cross-linking have been used to fabricate hydrogel materials. 13-14 Traditional chemical cross-linking

processes suffer severe drawbacks including harsh reaction conditions, longer reaction time and the potential toxicity of reactive substances, which has limited their application in biological fields. Click chemistry has emerged as powerful tool to synthesize 'soft hydrogels' owing to advantages such as high reaction speed, high selectivity and mild reaction conditions. A variety of click reactions has been used to synthesize materials for tissue engineering, including Diels—Alder and inverse electron demand Diels—Alder cycloaddition, azide—alkyne cycloadditions, thiol—ene/yne conjugation reactions as well as the Menschutkin click reaction 18-21. However, although much progress has been made in the field of coupling chemistries, the design of injectable hydrogels with elastic modulus high enough to provide sufficient structural support for tissue engineering applications remains a challenge.

Recent reports have demonstrated the inclusion of POSS into hydrogels to be a viable route towards improving biocompatibility and mechanical properties²²⁻²³. POSS can be thought of as 'molecular nanoparticle' with a symmetric cubic cage-like nanostructure, inherent nanoscale dimensions (about 0.5 nm in diameter) and multiple functionalities for chemical modification. These features render POSS nanoparticles versatile building blocks for organic-inorganic hybrid materials²⁴. Various kinds of POSS have been utilized to realize hybrid hydrogel networks with enhanced properties via chemical and physical crosslinking²⁵⁻²⁶. For example, PEG-POSS multiblock polyurethane hydrogels displayed higher stiffness than the according polyurethane hydrogels, in which the POSS nanocrystals serve as physical cross-linking points²⁷. Poly(2-hydroxyethyl methacrylate) (PHEMA)-based hydrogels with multimethacryloxy-POSS as a crosslinker were shown to improve surface properties, swelling behavior, and mechanical properties in the swollen state²⁸. POSS nanoparticles were also

introduced into poly(N-isopropyl acrylamide) (PNIPAM) gels as crosslinkers or microporogens to develop stimuli-responsive hydrogels. Zeng et al. prepared thermoresponsive POSS-containing PNIPAM hydrogels by using POSS with various long flexible chains. Using scanning probe microscopy the authors demonstrated the microstructure of hybrid hydrolgels to consist of hydrophobic nanodomains embedded within a cross-linked poly(N-isopropylacrylamide) (PNIPAAm) matrix.²⁹ Recently, a new step-growth process towards PEG hybrid hydrogel was demonstrated using *in situ* radical-mediated thiol–ene photopolymerization with octamethacrylate-POSS as crosslinker.³⁰ Octa(propylglycidyl ether)-POSS, mercapto-POSS, and octavinyl-POSS were also used in PNIPAAm gels to improve the response rate and mechanical properties^{25, 31-32}. In contrast, the development of POSS as a scaffold to enable injectable and degradable hydrogels with cleavable quaternary ammonium salt group for antibacterial activity has been rarely reported.

By extension of a previously reported click chemistry approach to facilitate embedding of POSS building blocks³³, we demonstrate a novel injectable and base-degradable POSS-based hybrid hydrogel with high antibacterial activity. In a first step, octa-ternary amino groups were introduced into commercial octavinyl POSS through a simple and rapid thiol-ene click reaction. Subsequent quaternarization of the functionalized POSS with chloroacetate derivatives resulted in POSS-based hybrid hydrogels with multiple QAS through pH-sensitive cleavable ester-linked bonds. The hybrid hydrogels exhibited a yield strength and elastic modulus of 0.36 MPa and 4.38 MPa. The antibacterial efficacy towards *Escherichia coli* and *Staphylococcus aureus* was 93% and 95 respectively. The hydrogel network was readily degraded under weak alkaline and at physiological conditions (pH = 7.4) to produce low toxic materials that retained

strong antibacterial activity.

EXPERIMENTAL SECTION

Materials. Octavinyl-T8-silsesquioxane (OV-POSS) was purchased from Hybrid Plastics Co. (America). 3-(Dimethylamino)-1-propanethiol (DPT) was purchased from Shenzhen Aituo Chemical Co., Ltd. (Shenzhen, China). 1-Hexadecanol and Benzoin dimethyl ether (DMAP) were purchased from Aladdin (Shanghai, China). 1,6-hexanediol and monochloroacetic acid were purchased from Shanghai Macklin Biochemical Co., Ltd (Shanghai, China). Tetrahydrofuran (THF) was dried over anhydrous MgSO₄. The other reagents were used as received.

Scheme 1. Synthetic route to the CCA, HBCA and OA-POSS.

Synthesis of the Octa-amino-POSS (OA-POSS)

The OA-POSS was synthesized following to previously reported methods³³. As shown in Scheme 1, Octavinyl POSS (OV-POSS) (0.63 g, 1 mmol) and 3-(Dimethylamino)-1-propanethiol (DPT) (1.19g, 10 mmol) were added into the dried THF (5 ml) in a Schlenk flask. The flask was wrapped with aluminum foil, and then the photoinitiator, DMPA (41 mg, 0.16 mmol), was added. After sealing, the mixture was purged with N₂ to eliminated oxygen. Then, aluminum foil was removed and the reaction was triggered by UV-irradiation at 365 nm under stirring at room temperature. As the reaction proceeded, OV-POSS gradually dissolved in the solution. After 1 h, the UV-light was turned off and the flask was connected to a distillation system. THF and excessive DPT were removed by vacuum evaporation at 30 °C, the resulting viscous liquid was the targeted product in quantitative yield. ¹H NMR (500 MHz, CDCl₃): 1.0 (t, Si-CH₂-CH₂-S, 2H), 1.65-1.84 (m, S-CH₂-CH₂-N, 2H), 2.16-2.26 (m, N(CH₃)₂, 6H), 2.30-2.36 (t, S-CH₂-CH₂-CH₂-N, 3H), 2.47-2.70 (m, Si-CH₂-CH₂-S, S-CH₂-CH₂-CH₂-N, 4H); ¹³C NMR (500 MHz, CDCl₃): 58.5, 45.3, 29.6, 27.3, 25.9, 12.9.

Synthesis of cetyl chloroacetate (CCA) and 1,6-hexanediol bis(chloroacetate) (HBCA)

The synthetic route to the CCA is shown in Scheme 1. A 250 ml round-bottom flask was charged with 1-hexadecanol (24.25 g, 0.10 mol), monochloroacetic acid (14.17g, 0.15mol) and *p*-toluenesulfonic acid (1.21g, 0.07mol) and toluene (100 ml). The mixture was heated to reflux with stirring for 12 h. After the reaction, a sodium hydroxide (NaOH) aqueous solution (1 M, 60 ml) was added into the reaction mixture to remove the excessive monochloroacetic acid. The organic phase was separated and washed with brine (50 ml). The organic phase was dried over anhydrous sodium sulfate, and then concentrated to afford CCA (28.07 g, 88%) as a white

solid. ¹H NMR (500 MHz, CDCl₃): 0.87-0.91 (t, C*H*₃ 3H), 1.27 ((C*H*₂)₁₃, 26H), 1.64-1.70 (m, C*H*₂, 2H), 4.07 (s, OOC-C*H*₂-Cl, 2 H), 4.18-4.21 (t, C*H*₂-OOC, 2H); ¹³C NMR (500 MHz, CDCl₃): 14.3, 22.1-32.4, 29.8, 42.5, 67.5, 167.3.

HBCA was prepared following the similar procedure for CCA (Scheme 1). 1,6-hexanediol (11.82 g, 0.1 mol), monochloroacetic acid (28.35 g, 0.3 mol), *p*-toluenesulfonic acid (2.41 g, 0.14 mol) and toluene (100 ml) were employed to give HBCA (23.58 g, 87%) as colorless liquid (Scheme 1). ¹H NMR (500 MHz, CDCl₃): 1.39-1.42 (m, CH₂-CH₂-CH₂-CH₂-CH₂-CH₂-CH₂, 4H), 1.66-1.72 (m, CH₂-CH₂-CH₂-CH₂-CH₂-CH₂-CH₂, 4H), 4.06 (s, CH₂Cl, 4H), 4.18-4.21 (t, CH₂-COC, 4H); ¹³C NMR (500 MHz, CDCl₃): 167.3, 67.3, 42.2, 28.3, 26.4.

Preparation of the hybrid hydrogels

In a 50 ml beaker, the prepared HBCA and CCA were dissolved in 0.8 ml isopropanol (IPA) under stirring. OA-POSS (0.8 g, 0.5 mmol) was then added into the prepared solution. After stirring for 10 minutes to get a homogeneous solution, the mixture was injected into a predesigned polytetrafluoroethylene mold (65 mm×20 mm×1.2 mm) by a syringe and the viscous mixture turned into a transparent organogel in less than 1 h. After mold removal, the POSS-based hybrid organogel was repeatedly immersed in IPA for three times to remove the unreacted reagents. Lastly, the POSS-based hybrid organogel was transferred and repeatedly soaked in deionized water for three times to remove the IPA solvents. After the IPA was completely replaced with water, the POSS-based hybrid hydrogel was obtained (Figure 5). The feed ratios of the various samples were presented in Table 1.

Table 1. Summary of feed ratios used for hybrid hydrogels.

Sample	OA-POSS	НВСА	CCA	Molar ratio of CCA/HBCA
POSS-HBCA4	0.8 g	0.54g	0	0
POSS- HBCA3-CCA2	0.8 g	0.41 g	0.45 g	0.7
POSS- HBCA2-CCA4	0.8 g	0.27 g	0.64 g	2
POSS- HBCA1-CCA6	0.8 g	0.14 g	0.96 g	6

Characterization

Chemical characterization was performed by ¹H NMR and ¹³C NMR spectroscopy using a Bruker AVANCE III 500 MHz. Chemical shifts were reported in parts per million (ppm) relative to the internal standards, partially deuterated solvents or tetramethylsilane (TMS). The structure of the dried hydrogel was characterized by Nicolet 6700 FTIR spectrophotometer (Thermo, USA), Lambda 950 ultraviolet-visible-near infrared absorption spectrum (UV–VIS–NIR) (Perkin-Elmer, USA) and X-ray photo-electron spectroscopy (XPS) (Axis Ultra, DLD, Kratos UK). Contact angles of the samples were characterized by means of OCA20 contact goniometer (Dataphysics, GER).

Compressive test

The mechanical properties of the hydrogels were tested by using a tensile-compressive tester (Instron 5996, Instron Co.). Before testing, the hydrogel was soaked in PBS (pH = 7.0) buffer. Each sample was allowed to swell to equilibrium. Hydrogel samples (16.8 mm diameter cylinder, the height is about 3.0 mm) were placed on the center of the lower compression plate. Then, the sample was compressed by the upper plate at a velocity of 1.0 mm min⁻¹. The maximum compression deformation was 30%, and the compressive strength and modulus were recorded. Each sample was conducted three times.

Swelling behavior of hydrogels

The swelling behavior of the hydrogel was evaluated by measuring the weight of swollen hydrogel (W_8) and freeze-dried hydrogel (W_0). A series of 0.2 g of the dried hydrogels were immersed in PBS (pH = 7.0) buffer at 25 °C. At regular intervals, the swollen hydrogel was wiped with wet filter paper to remove the residual water on the surface of hydrogels, and then the weight was measured. The swelling ratio (SR) was calculated according to the equation: $SR = (W_8 - W_0)/W_0$.

Hydrogel degradation

The hydrogel disks were incubated in a vial containing 5 ml PBS buffer (pH = 8.0 or 7.4) (or D_2O) and placed in a constant temperature oscillator (37 °C, 110 rpm). At pre-determined time points, a digital camera was taken to record the hydrolysis time of the sample. After the complete hydrolysis, the resulted hydrolysate in D_2O solution was characterized by ¹H NMR. *Antibacterial test*

Escherichia coli (E. coli, ATCC 25922) and Staphylococcus aureus (S. aureus) were chosen as model bacteria to study the antibacterial property of the hydrogel samples at physiological conditions. A single colony of each bacteria was used to inoculate 20 ml of Luria-Bertani (LB) liquid culture (pH = 7.4) separately. After incubated overnight at 37 °C with shaking, the cultures were diluted to the optical density of \sim 0.1 (E. coli) and \sim 0.05 (S. aureus) at 600 nm with LB (the bacteria densities are 2.53×10^7 cfu/ml and 1.14×10^7 cfu/ml for E.coli and S. aureus, respectively). The hydrogel was placed in a twelve-well plate containing 3 ml bacteria and incubated for 37 °C for a certain time (E. coli 24 h) and (S. aureus 12 h). Finally, the samples were washed with PBS buffer to remove the non-adherent bacteria. Bacteria adhering

on the surface of the hydrogel were dyed by dropping diluted Live/Dead BackLight Kit (Thermo Fisher Scientific Inc., NY) and observed with an Axio Observer (Carl Zeiss Jena., OBSERVER) inverted fluorescence microscope under a 40-fold objective lens.

Determination of minimum inhibitory concentration (MIC) of the hydrogel hydrolysate

The minimum inhibitory concentration (MIC), the lowest concentration of the applied material that can inhibit the growth of an organism, was determined by using the batch cultures containing different volumes of the hydrolysate of the hydrogels. *E. coli* and *S. aureus* were also chosen. A single colony of each bacteria was used to inoculate 20 ml of LB (pH = 7.4) separately. After incubated overnight at 37 °C with shaking, the cultures were diluted to the optical density of ~ 0.1 (*E. coli*) and ~ 0.05 (*S. aureus*) at 600 nm with LB (the bacteria densities are 2.53×10^7 cfu/ml and 1.14×10^7 cfu/mL for *E. coli* and *S. aureus*, respectively), then diluted 100 times with diluted culture solution to make the concentration of bacteria around $1-3 \times 10^6$

cfu·mL⁻¹.

The MIC of the aqueous solution of hydrogels was determined by two-fold dilution method. A LB liquid culture (2 ml) was poured into the each well of the 12-well plate. Then 2 ml hydrolysate (1 g/ml) of the hydrogel was added into the first well with a pipette gun. After homogeneous mixing, 2 ml of the mixture was taken out from the first well and added into the second well etc. until the 11th well; 2 ml of the mixture was taken out of the 11th well, so the concentration from 1 to 10 wells is diluted twice in turn. The 11th well was the control sample with 2 mL LB liquid medium, and then 0.1 ml of diluted bacterial solution was added into each well. After being incubated at 37 °C for 24 h, a digital camera was used to record the experimental results. When the solution was clear, there was no large amount of bacterial

growth. When the solution was turbid, it was bacterial growth. MIC was calculated based on the viable colony count method. Each experiment was carried out in triplicate.

RESULTS AND DISCUSSION

OA-POSS with eight dimethylamino groups was synthesized by thiol-ene click chemistry³³. Under UV-irradiation, 3-(dimethylamino)-1-propanethiol was found to react rapidly with OV-POSS in quantitative yield to OA-POSS. Monochloroacetic acid reacted with fatty alcohol (1-hexadecanol and 1,6-hexanediol) to form cetyl chloroacetate (CCA) and 1,6-hexanediol bis(chloroacetate) (HBCA), respectively. Their purity and chemical structures were confirmed by ¹H- and ¹³C-NMR spectroscopy (see Supporting Information, Fig. S1-S6). The chemical structure of the gels was characterized by means of FT-IR spectroscopy.

From Figure S7, it can be seen that peaks at 2958 cm⁻¹ and 2864 cm⁻¹ were ascribed to the symmetric and asymmetric vibrations of the -CH₂- groups of the alkyl chains in the HBCA, respectively. The peak centered at 1470 cm⁻¹, was assigned to the bending vibration of -CH₂-moiety. Further, a band at 720 cm⁻¹ (a characteristic absorption peak of long carbon chains - $(CH_2)_n$ - for $n \ge 4$) was also observed. In addition, peaks at 1470 and 1186 cm⁻¹ were ascribed to the stretching vibration of the carbonyl (C=O) group and the C-O-C stretching vibration in the ester bond, respectively. Similar bands were observed for CCA (Fig. S7). After Menschutkin click reactions, taking POSS-HBCA4 for an example, quarternization to OA-POSS was confirmed by a new peak at 1129.8 cm⁻¹ (Fig. 1) that could be assigned to the Si-O-Si stretching vibration of the POSS cage, the disappearance of the peak at 789 cm⁻¹ (indicating the cleavage of the C-Cl bond) as well as a new band near 910 cm⁻¹ (Fig. 1) corresponding to

the stretching vibration of the -C-N⁺- group. The reaction triggered the formation of the hybrid hydrogel.

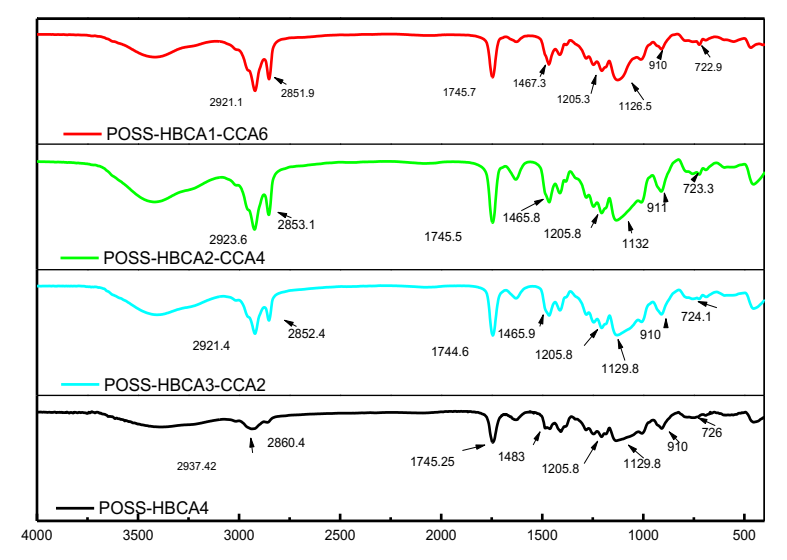


Figure 1. FT-IR spectra of hybrid hydrogels. See text for more details.

To further confirm the structure of the hydrogels, XPS analysis was-performed. Figure 2 displays the XPS spectrum of the hydrogel revealing bands at 194.4 eV and 399 eV due to Cl_{2p} and N_{1s} transitions, respectively (Fig. 2). The Cl_{2p} band can be deconvoluted into two peaks with binding energies at 194.4 and 196.3 eV, which correspond to the 2p orbital spin double spectral line of Cl. The peak at 399 eV was attributed to the N_{1s} (corresponding to the quaternary ammonium salt group) thus confirming the Menschutkin reaction. The spectra further revealed that the C-content within the hydrogel surface increased with the molar ratio of CCA/HBCA. The C atomic content of POSS-HBCA4, POSS-HBCA3-CCA2, POSS-HBCA2-CCA4 and POSS-HBCA1-CCA6 was 63.8%, 72.13%, 76.74% and 80.29% respectively (see Table S1 in Supporting Information).

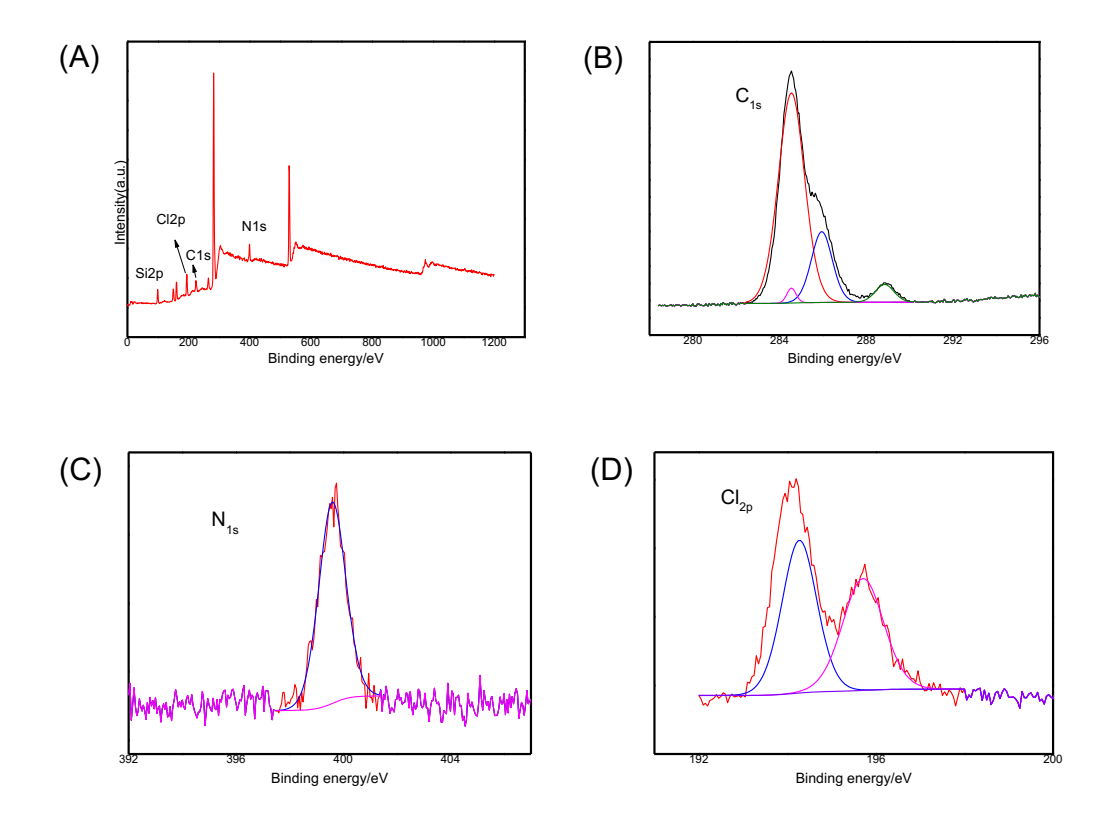


Figure 2. Wide region XPS spectra of the hybrid hydrogel (POSS-HBCA3-CCA2) revealing C_{1s} (B), N_{1s} (C), and Cl_{2p} (D) peaks in XPS spectra.

The swelling behavior of the hybrid hydrogels with different molar ratios of CCA/HBCA in PBS buffer solution (pH = 7.0) is depicted in Figure 3. The swelling ratio SR (calculated as SR = $(Ws - W_0)/W_0$, where Ws denotes the weight of swollen hydrogel and W_0 the weight of the freeze-dried hydrogel) rapidly increased with time of immersion, ultimately levelling off at the equilibrium swelling ratio. The equilibrium swelling ratio of the POSS-HBCA3-CCA2, POSS-HBCA2-CCA4 and POSS-HBCA1-CCA6 sample was 300%, 500% and 800%, respectively. This suggests that the increase of the molar fraction of the CCA/HBCA resulted in the increase of the number of crosslinking points in the hydrogel network, thus facilitating more pronounced swelling. Independent of the crosslink density, the equilibrium swelling ratio was observed after about 48 hours. The short equilibrium swelling time was attributed to the high concentration of quaternary ammonium groups in the hybrid hydrogel networks that increase

the osmotic driving force for swelling.

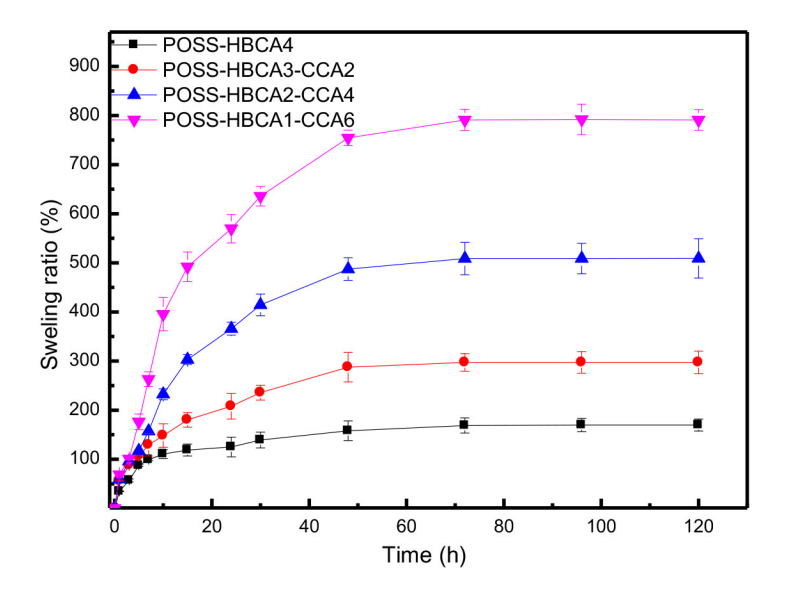


Figure 3. Plot of the swelling kinetics of the various hydrogels in PBS buffer solution (pH = 7.0). The equilibrium swelling fraction increases with molar fraction of CCA/HBCA. Swelling is completed after 48 h independent of the equilibrium swelling ratio.

The static water contact angle on the surface of the hybrid hydrogels with different molar ratio of the CCA/HBCA were measured with an automatic optical contact angle tester. The optical images of the water contact angle on the various hydrogel samples are presented in Figure S8. The contact angle of the POSS-HBCA4 sample was only 88°, smaller than 90°, indicating more hydrophilic behavior (Fig. 4). However, the contact angle of the POSS-HBCA3-CCA2, POSS-HBCA2-CCA4 and POSS-HBCA1-CCA6 sample increased to 100°, 108° and 113°, respectively (Fig. 4). This indicated that the hydrophobicity of the hybrid hydrogels increased with the molar ratio of the CCA/HBCA. We hypothesized that the increase of contact angle was due to the enrichment of the hydrophobic alkyl and ester groups in the proximity of the surface. This supports that the C atomic content at (and near) the hydrogel surface increases with the ratio of CCA/HBCA (Table S1 in Supporting Information). This is relevant because, the higher density of hydrophobic long-chain alkyl groups on the outer surface could raise the

number of QAS groups contacting bacteria, which may benefit the killing efficiency towards bacteria.

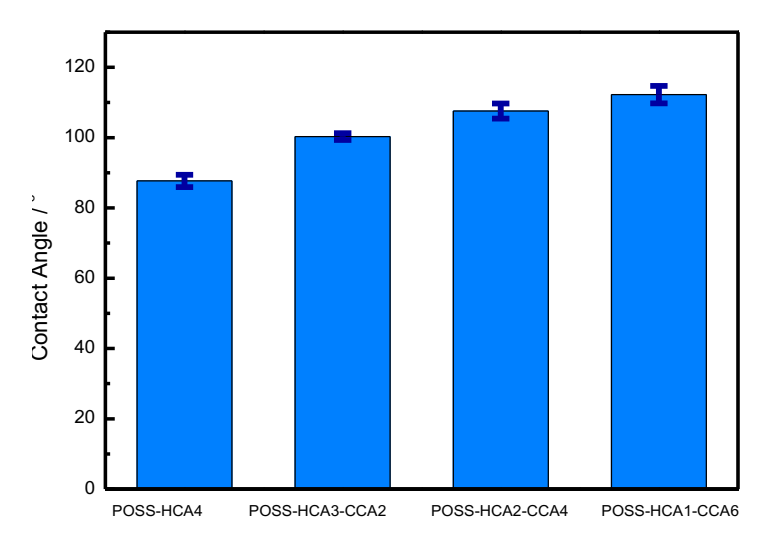


Figure 4. Static contact angles of the dried hybrid hydrogels as determined by ellipsometry. Hydrophobicity (indicated by increasing contact angle) increases with HBCA content.

The mechanical strength of hydrogels is an important parameter in applications such as implants materials and medical dressings. Previous work has shown that the introduction of POSS into hydrogel networks can improve the mechanical strength of the hydrogel materials²⁴. As shown in Figures 5C-F, the POSS-HBCA3-CCA2 hydrogel sample exhibited good flexural and torsional stability and displayed full recovery after unloading.

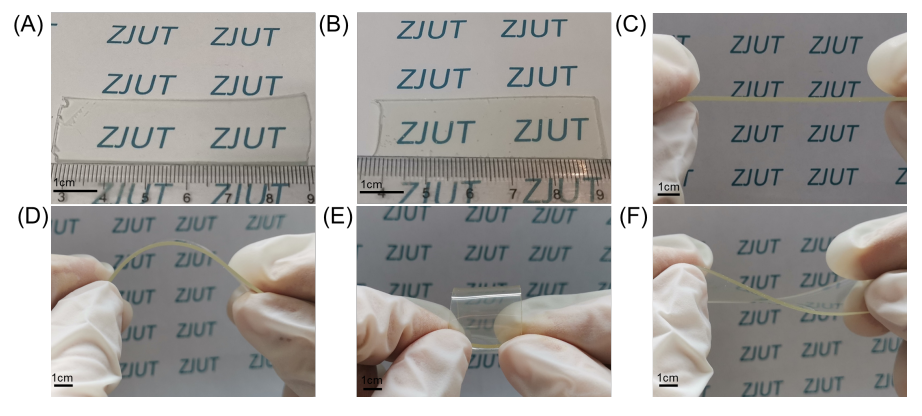


Figure 5. Photographs of the hybrid hydrogels undergoing twist-torsion deformation. Panel (A) and (B) are POSS-HBCA4 and POSS-HBCA1-CCA6, respectively. Panel (C), (D), (E) and (F) are different forms of POSS-HBCA3-CCA2, respectively.

The mechanical properties of hybrid hydrogels were investigated by tensile compression. Figure 6A displays the compressive stress-strain curves of hybrid hydrogels with different molar ratio of CCA/HBCA. At compressive strains below 10% the response of the materials was predominantly elastic (as confirmed by the linear stress-strain relation). Larger compressive strains (10-20%) exhibited nonlinear behavior, ultimately resulting in the sharp increase of the compressive stress when the compressive strain reached 20-30%. During the unloading process, strain hysteresis was observed and attributed to a time-delayed elastic response since all hydrogels eventually displayed complete shape recovery.

The results of compression testing are shown in Figure 6B. The figure reveals that the compressive stress and the compression modulus of the hybrid hydrogel decreased continuously with increasing molar ratio of CCA/HBCA. For example, the yield stress of POSS-HBCA4 was 0.36 MPa whereas the yield stress of POSS-HBCA3-CCA2, POSS-HBCA2-CCA4 and POSS-HBCA1-CCA6 sample was 0.24, 0.16 and 0.09 MPa under 30% deformation, respectively. The compressive (elastic) modulus of the hybrid hydrogels displayed a similar trend. The compression modulus of POSS-HBCA4, POSS-HBCA3-CCA2, POSS-HBCA2-CCA4 and POSS-HBCA1-CCA6 was 4.38, 3.9, 1.2 and 0.4 MPa, respectively. We interpreted this trend as a consequence of a decreasing crosslink density with HBCA content. This allowed for the controlled variation of the mechanical strength of hybrid hydrogel could by modulation of the molar ratio of CCA/HBCA.

The mechanical strength of the hydrogels after multiple loading-unloading cycles has been examined to evaluate the stability and durability of the hydrogel samples. The maximum load of the tested hydrogels decreased slightly with increasing the loading-unloading cycles but the

change was rather small (Fig. S9). Again, considering POSS-HBCA4 as an example, the original maximum load was ~62 N (Fig. S9A). Only a small decrease of the maximum load was observed when the number of loading-unloading cycles increased. However, the maximum load was almost constant at ~55 N even after 50 loading-unloading cycles, as evidenced by only ~10% decrease. The above results confirmed the stability of the network structure of hydrogels during the loading/unloading process. Thus, the hydrogels had good elasticity and shape recovery ability.

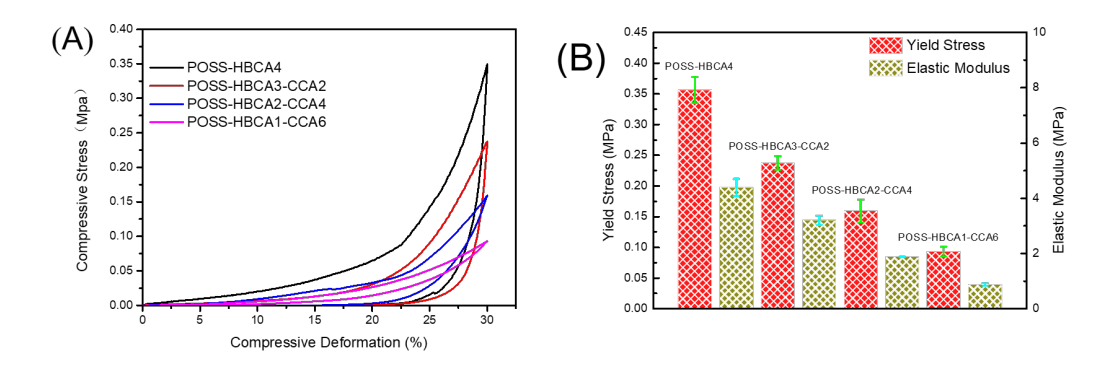


Figure 6. (A) Compression deformation stress diagram of the hybrid hydrogels (B) Yield stress and elastic modulus of the hybrid hydrogels (yield stress is defined as stress at 30% deformation strain).

E. coli (Gram-negative) and *S. aureus* (Gram-positive) were used as the model bacteria to test the antibacterial properties of the hybrid hydrogels. As shown in Figure 7 and Figure 8, the concentration of the *E. coli* attached on the surface of the POSS-HBCA4 was the highest (Fig. 7A), up to 5.3×10⁵ cfu/cm² (Fig. 8A). With increasing molar fraction of CCA in the hydrogel network, the density of the attached *E. coli* on the hydrogel decreased significantly (Fig. 7C and 7D). For example, the density of bacteria on the POSS-HBCA3-CCA2, POSS-HBCA2-CCA4, POSS-HBCA1-CCA6 hydrogel sample was determined as 3.2×10⁵, 2.4×10⁵, 2.1×10⁵ cfu/cm², respectively (Fig. 8A), indicating that the long alkyl chain played a significant role in

improving the bacterial resistance. Importantly, the killing rate of the hybrid hydrogels also increased with the increase of CCA in the hydrogel network. The POSS-HBCA4 hydrogel sample was found to only kill 69% E. coli, while the killing efficiency of the POSS-HBCA1-CCA6 hydrogel increased to 93% (Fig. 8B). When quarternary ammonium salt cation groups were combined with the long alkyl group, the hydrophobic alkyl could facilitate the quarternary ammonium salt penetrating the cell membrane and kill the bacteria³⁴⁻³⁵. The observed trend supports previous reports by Salton et al. who proposed that the mechanism for antibacterial action involves the adsorption of QACs and the subsequent reduction of structural integrity of the cytoplasmic membrane in bacteria³⁶⁻³⁷. A similar mechanism might be responsible for the observed trend. Compared with the antibacterial effect on E. coli, the number of adhered S. aureus on the hybrid hydrogel was larger. The amount of the S. aureus attached on the surface of the POSS-HBCA4 was up to 2.0×10^6 cfu/cm² (Fig. S9, 10). Similarly, with increasing of CCA, the attached S. aureus on the hydrogel decreased greatly (Fig. S10, 11). However, the hybrid hydrogel showed better antibacterial efficacy on S. aureus (gram positive). The POSS-HBCA2-CCA4 and POSS-HBCA1-CCA6 hydrogel sample could kill almost ~100% of S. aureus (Fig. 8B), thus indicating excellent bacterial-killing activity.

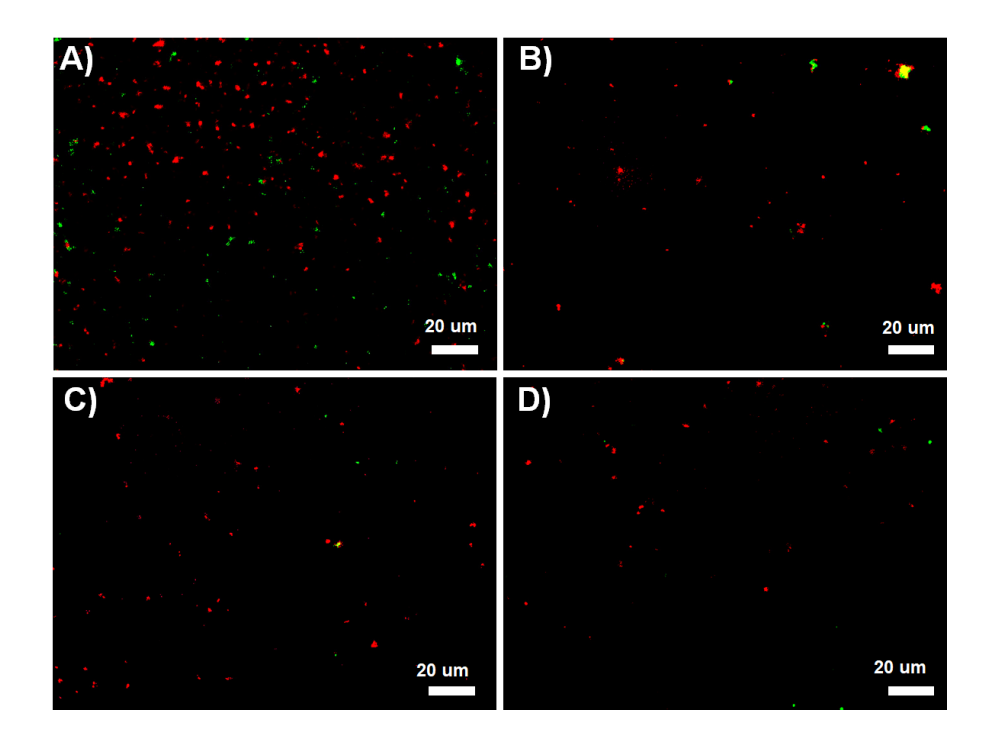


Figure 7. Confocal images of *E. coli* adhered on the various hydrogel surfaces, where A), B), C) and D) are the POSS-HBCA4, POSS-HBCA3-CCA2, POSS-HBCA2-CCA4 and POSS-HBCA1-CCA6, respectively. Scale bars are 20 μm.

It was reported that the cationic charge close to the ester bond renders normal ester quants unusually stable to acid and labile to alkali.³⁸ The strong pH dependence of the hydrolysis was advantageous for the rapid cleavage of the product. This phenomenon was even more pronounced for betaine esters.^{39,40} Such esters undergo alkaline hydrolysis at a much faster rate than esters lacking the adjacent charge. The large effect on the rate of alkaline and acid hydrolysis of the quaternary ammonium group is due to stabilization/destabilization of the ground state. The charge repulsion, involving the carbonyl carbon atom and the positive charge at the nitrogen atom, is relieved by hydroxide ion attack, but augmented by protonation.³⁸⁻⁴⁰ Compared with ester lacking the cationic charge, the rate of alkaline hydrolysis is increased 200-fold, whereas the rate of acid hydrolysis is decreased 2000-fold.⁴¹ Since the hydrogel in this work has a similar chemical structure as the previously reported ester quants, the rapid hydrolysis under weak alkaline conditions is in good agreement with the previously reported results.

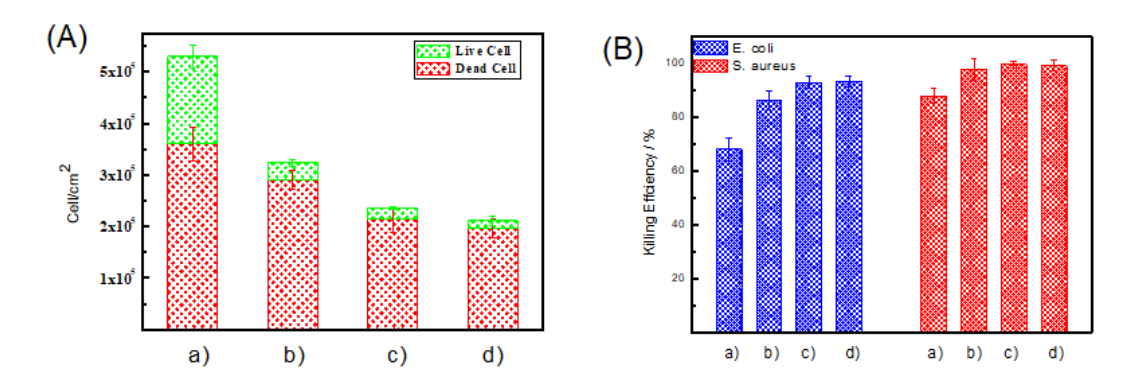


Figure 8. A) the quantitative statistics for *E. coli* and B) the killing efficiency of the various hydrogel towards *E. coli* and *S. aureus*; where a), b), c) and d) are the POSS-HBCA4, POSS-HBCA3-CCA2, POSS-HBCA2-CCA4 and POSS-HBCA1-CCA6, respectively.

Hydrogel containing quarternary ammonium salts have been shown to be effective against a variety of bacteria⁴². However, a common challenge is the adhesion of dead microorganisms that can trigger immune response and inflammation. In this work, the quarternary ammonium groups were crosslinked into the hydrogel network through cleavable betaine ester bonds, which was expected to prevent the biofilm by degradation of the hydrogel. In this case, a tightly bound water layer around hydrophilic chains is expected to induce large repulsive hydration forces^{43,44}. In addition, the strong binding of the hydration layer of zwitterionic materials promotes ultra-low-fouling ^{45,46}. As shown in Figure S12, the hydrogel gradually hydrolyzed when being immersed into a weak alkaline PBS buffer (pH = 8). For example, the volume of POSS-HBCA4 hydrogels continuously decreased and the solution became visibly turbid after immersion in PBS buffer for 36 h, indicating the hydrolysis of the hydrogel. After 48 h hydrolysis was found to be complete. The degradation is favored by the quarternary ammonium group adjacent to ester bonds that exert a strong electron-withdrawing effect^{41,47}, thus reducing the activation energy of the hydrolysis. From Figure 9, the hydrolysis time had a close relationship with the molar ratio of the CCA/HBCA. The hydrolysis time of the PO Kinetics of

the acid and alkaline hydrolysis of ethoxycarbonylmethyltriethylammonium chloride SS-HBCA4, POSS-HBCA3-CCA2, POSS-HBCA2-CCA4 and POSS-HBCA1-CCA6 hydrogel was 48, 36, 24 and 6 h respectively. This might be caused by the decrease of the crosslink density with increasing of the molar ratio of the CCA which should promote the degradation of the hydrogel.

We further studied the hydrolysis of the hydrogel samples in PBS buffer at physiological conditions (pH = 7.4). As shown in Figure S13, the tested hydrogel samples were gradually swollen when being immersed into at physiological conditions. The hydrolysis behavior of the hydrogels at physiological conditions was similar with that under a weak alkaline PBS buffer (pH = 8). The hydrolysis time of the hydrogel sample was greatly decreased with increased ratio of the CCA/HBCA at physiological conditions. The hydrolysis time of the POSS-HBCA4, POSS-HBCA3-CCA2, POSS-HBCA2-CCA4 and POSS-HBCA1-CCA6 hydrogel was 984, 744, 456 and 168 h (Fig. S14), respectively. However, the hydrolysis time of the hydrogels at physiological conditions (pH = 7.4) was much longer than that under weak alkaline conditions (pH = 8.0). For example, the hydrolysis time of the POSS-HBCA4 was only 48 h in PBS buffer under a weak alkaline condition (pH = 8.0). In contrast, the POSS-HBCA4 needed 984 h to fully hydrolyze in PBS buffer at physiological conditions (pH = 7.4). Therefore, the hydrogel samples are expected to maintain excellent antibacterial characteristics at physiological conditions.

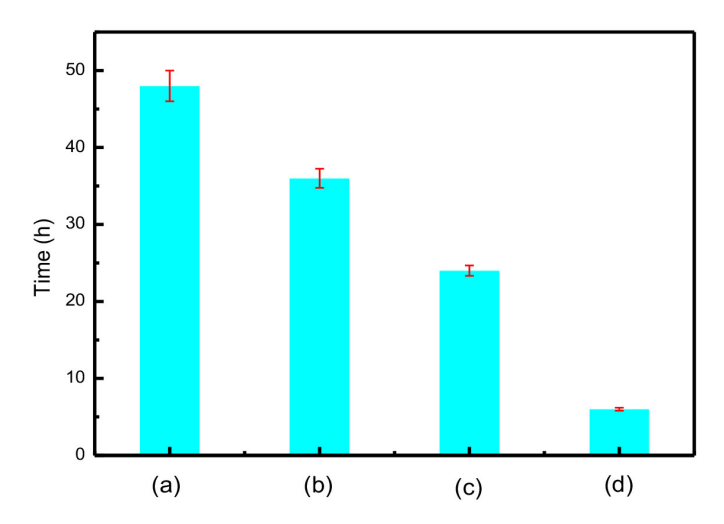


Figure 9. the complete hydrolysis time of the various hydrogels in PBS buffer (pH = 8.0), where (a), (b), (c) and (d) correspond to POSS-HBCA4, POSS-HBCA3-CCA2, POSS-HBCA2-CCA4 and POSS-HBCA1-CCA6 hydrogel samples, respectively.

The degradation of POSS-HBCA4 was further studied by 1 H NMR to elucidate the mechanism of degradation. After complete degradation, the hydrogel network was resolved to produce 1,6-hexanediol and POSS-functionalized zwitterionic carboxybetaines. From Figure 10, the chemical shifts of the COO-C H_2 - in the HBCA was 3.9 ppm. After degradation, the H_h chemical shifts of the O-C H_2 - in the 1,6-hexanediol were shifted upfield to 3.4 ppm. Similarly, the protons of the CIC H_2 COO group showed significant upfield shift (from 3.8 ppm (Fig. S5) to 3.1 ppm (H_g)). Conversely, the peak at 2.2 ppm ascribed to N-C H_3 in the OA-POSS (Fig. S1) shifted downfield (0.9 ppm) after hydrolysis due to the stronger electron-withdrawing effect of the resulting ammonium ions. In addition, the protons (-C H_2 N-) of the OA-POSS also showed a considerable downfield-shift (\sim 1.1 ppm) after degradable process. These results indicated that the hydrogel networks could be gradually degradable under the basic environment due to the hydrolysis of the ester group under the basic environment.

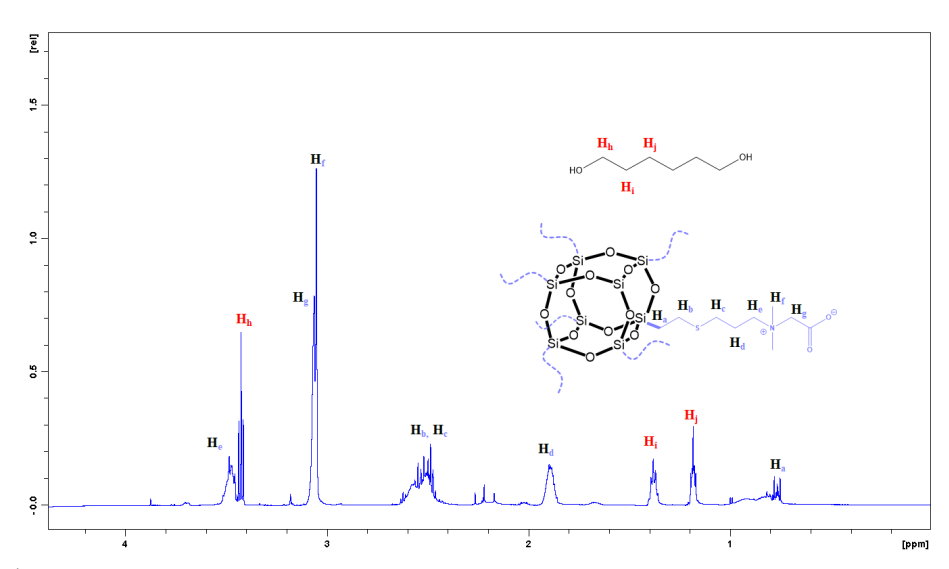


Figure 10. ¹H NMR spectra of the hydrolysate of the POSS-HBCA4 sample in D₂O.

To evaluate the antibacterial effect of the hydrolysate of the hydrogel, a minimum inhibitory concentration (MIC) test was conducted. As shown in Table 2, the MIC of the POSS-HBCA4 hydrolysate against *E. coli* and *S. aureus* is 5000 μg ml⁻¹. In contrast, the MIC of the hydrolysate of the hydrogel containing CCA towards *E. coli* and *S. aureus* significantly deceased. The MIC of the hydrolysates of the POSS-HBCA3-CCA2, POSS-HBCA2-CCA4 and POSS-HBCA1-CCA6 against *E. coli* was 156.25, 156.25 and 39.06 μg ml⁻¹, respectively. Compared with *E. coli*, the MIC of the hydrolysates of the hydrogels against *S. aureus* was much smaller. The MIC of the hydrolysates of the POSS-HBCA3-CCA2, POSS-HBCA2-CCA4 and POSS-HBCA1-CCA6 was as low as 9.77μg ml⁻¹. The antibacterial activity of the hydrolysate was consistent with that of the hydrogel. Therefore, the hydrogel and the hydrolysates both showed efficient antibacterial properties. Thus, the antibacterial properties of these hydrogel materials are expected to be long-term effective at physiological conditions.

Table 2. The minimum inhibitory concentration (MIC) of the hydrolysate of the hydrogels after complete hydrolysis

Sample Conc. / μg mL ⁻¹	POSS-HBCA4	POSS-HBCA3-CCA2	POSS-HBCA2-CCA4	POSS-HBCA1-CCA6
E.coli	5000	156.25	156.25	39.06
S.aureus	5000	9.77	9.77	9.77

CONCLUSIONS

A series of cross-linked POSS hydrogel networks containing betaine ester groups was synthesized using thiol-ene click chemistry and subsequent reaction of amino functionalities with chloroacetate derivatives. Upon immersion in PBS buffer, all hydrogels displayed rapid swelling and an ultimate equilibrium swelling ratio of up to 800%. The contact angle of hybrid hydrogels increased from 88° to 113° with increasing molar ratio of CCA/HBCA, thus suggesting the enrichment of hydrophobic alkyl and ester groups on the hydrogel surface. The hybrid hydrogels exhibited excellent mechanical robustness towards tensile, bend and torsional deformation. For E. coli and S. aureus, the hybrid hydrogels displayed high antibacterial activity. Increasing the content of cetyl chloroacetate (CCA) in the hydrogel network resulted in higher killing rate of the hydrogels, presumably caused by the higher concentration of long alkyl betaine ester. The hydrogel could be hydrolyzed under weak alkaline conditions and at physiological conditions; the hydrolysis time increased with increasing concentration of CCA in the hydrogel. The hydrolysis time of the hydrogels at physiological conditions was much longer than that under weak alkaline conditions. The minimum inhibitory concentration (MIC) of the hydrolysate towards E. coli and S. aureus was 39.1 and 9.77 µg ml⁻¹, respectively. The combination of favorable features, such as synthetic versatility, robust mechanical properties,

antibacterial activity and tunable degradation characteristics could render these hybrid hydrogels interesting candidates in areas such as tissue engineering or for interface modification.

ASSOCIATED CONTENT

Supporting information. ¹H NMR spectra of OA-POSS (Fig. S1); ¹³C NMR spectra of OA-POSS (Fig. S2); ¹H NMR spectra of CCA (Fig. S3); ¹³C NMR spectra of CCA (Fig. S4); ¹H NMR spectra of HBCA (Fig. S5); ¹³C NMR spectra of HBCA (Fig. S6); FT-IR spectra of CCA and HBCA (Fig. S6); Hydrolysis of the hybrid hydrogel in PBS buffer under weak alkaline conditions (pH = 8.0) over time (Fig. S7); Surface element composition of the various hybrid hydrogels (Table S1).

ACKNOWLEDGEMENTS

The authors gratefully acknowledge the financial support of the National Nature Science Foundation (51303192, 51603217), the Ningbo Major Special Project (2013B6012), and Scholarship of CSC (201808330007), Scientific and Technological Innovation Programs of Higher Education Institutions in Shanxi (2019L0739) and Innovation & Application Engineering Research Center for Mesoporous Materials (MMIA2019101). MRB acknowledges financial support by the National Science Foundation via award DMR-1709344.

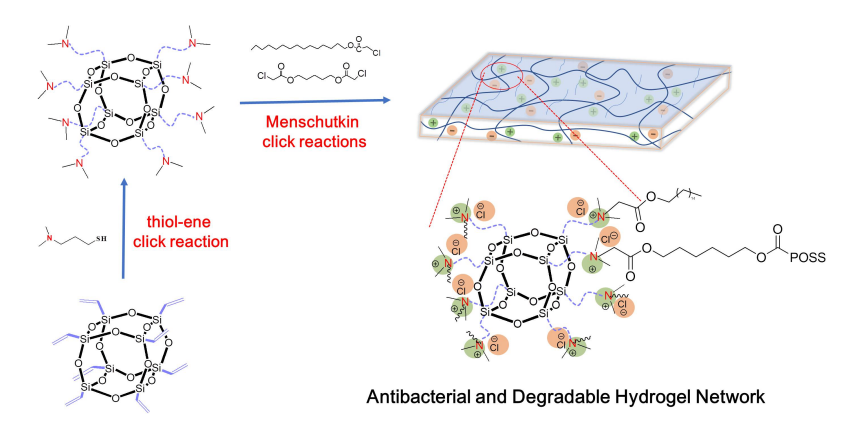
REFERENCES

- 1. Culver, H. R.; Clegg, J. R.; Peppas, N. A., Analyte-responsive hydrogels: Intelligent materials for biosensing and drug delivery. *Acc. Chem. Res.* **2017**, *50* (2), 170-178.
- 2. Lee, K. Y.; Mooney, D. J., Hydrogels for Tissue Engineering. Chem. Rev. 2001, 101 (7), 1869-1880.
- 3. Sood, N.; Bhardwaj, A.; Mehta, S.; Mehta, A., Stimuli-responsive hydrogels in drug delivery and tissue engineering. *Drug Deliv.* **2016**, *23* (3), 748-770.
- 4. Nam, S.; Stowers, R.; Lou, J.; Xia, Y.; Chaudhuri, O., Varying PEG density to control stress relaxation in alginate-PEG hydrogels for 3D cell culture studies. *Biomaterials* **2019**, *200*, 15-24.
- 5. Matricardi, P.; Alhaique, F.; Coviello, T., *Polysaccharide hydrogels: Characterization and biomedical applications.* CRC Press: 2016.
- 6. Wu, J.; Xiao, Z.; Chen, A.; He, H.; He, C.; Shuai, X.; Li, X.; Chen, S.; Zhang, Y.; Ren, B., Sulfated zwitterionic poly (sulfobetaine methacrylate) hydrogels promote complete skin regeneration. *Acta Biomater.* **2018**, *71*, 293-305.
- 7. Bryant, S. J.; Anseth, K. S., Hydrogel properties influence ECM production by chondrocytes photoencapsulated in poly(ethylene glycol) hydrogels. *J. Biomed. Mater. Res.* **2002**, *59* (1), 63-72.
- 8. Xu, W.; Dong, S.; Han, Y.; Li, S.; Liu, Y., Hydrogels as antibacterial biomaterials. *Curr. Pharm. Design* **2018**, *24* (8), 843-854.
- 9. Hu, H.; Xu, F.-J., Rational design and latest advances of polysaccharide-based hydrogels for wound healing. *Biomater. Sci.* **2020**, *8* (8), 2084-2101.
- 10. Thorsteinsson, T.; Másson, M.; Kristinsson, K. G.; Hjálmarsdóttir, M. A.; Hilmarsson, H.; Loftsson, T., Soft antimicrobial agents: synthesis and activity of labile environmentally friendly long chain quaternary ammonium compounds. *J. Med. Chem.* **2003**, *46* (19), 4173-4181.
- 11. Wang, W.; Lu, Y.; Zhu, H.; Cao, Z., Superdurable Coating Fabricated from a Double-Sided Tape with Long Term "Zero" Bacterial Adhesion. *Adv. Mater.* **2017**, *29* (34).
- 12. Wang, Z.; Scheres, L.; Xia, H.; Zuilhof, H., Developments and Challenges in Self-Healing Antifouling Materials. *Adv. Funct. Mater.* **2020**.
- 13. Nezhad-Mokhtari, P.; Ghorbani, M.; Roshangar, L.; Rad, J. S., A review on the construction of hydrogel scaffolds by various chemically techniques for tissue engineering. *Eur. Polym. J.* **2019**, *117*, 64-76.
- 14. Hu, W.; Wang, Z.; Xiao, Y.; Zhang, S.; Wang, J., Advances in crosslinking strategies of biomedical hydrogels. *Biomater. Sci.* **2019**, *7* (3), 843-855.
- 15. Xu, Z.; Bratlie, K. M., Click Chemistry and Material Selection for in Situ Fabrication of Hydrogels in Tissue Engineering Applications. *ACS Biomater. Sci. Eng.* **2018**, *4* (7), 2276-2291.
- 16. Konai, M. M.; Bhattacharjee, B.; Ghosh, S.; Haldar, J., Recent Progress in Polymer Research to Tackle Infections and Antimicrobial Resistance. *Biomacromolecules* **2018**, *19* (6), 1888-1917.
- 17. Gopinathan, J.; Noh, I., Click Chemistry-Based Injectable Hydrogels and Bioprinting Inks for Tissue Engineering Applications. *Tissue Eng. Regen. Med.* **2018**, *15* (5), 531-546.
- 18. Murakami, T.; Brown, H. R.; Hawker, C. J., One-pot fabrication of robust interpenetrating hydrogels via orthogonal click reactions. *J. Polym. Sci. Part A: Polym. Chem.* **2016**, *54* (11), 1459-1467.
- 19. Anseth, K. S.; Klok, H.-A., Click chemistry in biomaterials, nanomedicine, and drug delivery. *Biomacromolecules* **2016**, *17* (1), 1–3.
- 20. Wang, X.; Li, Z.; Shi, T.; Zhao, P.; An, K.; Lin, C.; Liu, H., Injectable dextran hydrogels fabricated by metal-free click chemistry for cartilage tissue engineering. *Mat. Sci. Eng. C* **2017**, *73*, 21-30.
- 21. Zhang, Y.; Liu, S.; Li, T.; Zhang, L.; Azhar, U.; Ma, J.; Zhai, C.; Zong, C.; Zhang, S.,

- Cytocompatible and non-fouling zwitterionic hyaluronic acid-based hydrogels using thiol-ene "click" chemistry for cell encapsulation. *Carbohydr. Polym.* **2020,** *236*, 116021.
- 22. Pu, W.; Jiang, F.; Chen, P.; Wei, B., A POSS based hydrogel with mechanical robustness, cohesiveness and a rapid self-healing ability by electrostatic interaction. *Soft Matter* **2017**, *13* (34), 5645-5648.
- 23. Zhang, X.; Li, C.; Hu, Y.; Liu, R.; He, L.; Fang, S., A novel temperature and pH dual-responsive hybrid hydrogel with polyhedral oligomeric silsesquioxane as crosslinker: synthesis, characterization and drug release properties. *Polym. Int.* **2014**, *63* (12), 2030-2041.
- 24. Kuo, S.-W.; Chang, F.-C., POSS related polymer nanocomposites. *Prog. Polym. Sci.* **2011,** *36* (12), 1649-1696.
- 25. Wang, J.; Sutti, A.; Wang, X.; Lin, T., Fast responsive and morphologically robust thermoresponsive hydrogel nanofibres from poly (N-isopropylacrylamide) and POSS crosslinker. *Soft Matter* **2011**, *7* (9), 4364-4369.
- 26. Haldar, U.; Nandi, M.; Maiti, B.; De, P., POSS-induced enhancement of mechanical strength in RAFT-made thermoresponsive hydrogels. *Polym. Chem.* **2015**, *6* (28), 5077-5085.
- 27. Wu, J.; Ge, Q.; Mather, P. T., PEG- POSS multiblock polyurethanes: synthesis, characterization, and hydrogel formation. *Macromolecules* **2010**, *43* (18), 7637-7649.
- 28. Prządka, D.; Andrzejewska, E.; Marcinkowska, A., Multimethacryloxy-POSS as a crosslinker for hydrogel materials. *Eur. Polym. J.* **2015,** *72*, 34-49.
- 29. Zeng, K.; Wang, L.; Zheng, S., Rapid Deswelling and Reswelling Response of Poly(N-isopropylacrylamide) Hydrogels via Formation of Interpenetrating Polymer Networks with Polyhedral Oligomeric Silsesquioxane-Capped Poly(ethylene oxide) Amphiphilic Telechelics. *J. Phys. Chem. B* **2009**, *113* (35), 11831-11840.
- 30. Alves, F.; Nischang, I., A simple approach to hybrid inorganic–organic step-growth hydrogels with scalable control of physicochemical properties and biodegradability. *Polym. Chem.* **2015**, *6* (12), 2183-2187.
- 31. Chen, Y.; Xiong, Y.; Peng, C.; Liu, W.; Peng, Y.; Xu, W., Synthesis and characterization of POSS hybrid co-cross-linked p (NIPA-co-DMAEMA) hydrogels. *J. Polym. Sci. Part B: Polym. Phys.* **2013**, *51*, 1494-1504.
- 32. Xu, Z.; Ni, C.; Yao, B.; Tao, L.; Zhu, C.; Han, Q.; Mi, J., The preparation and properties of hybridized hydrogels based on cubic thiol-functionalized silsesquioxane covalently linked with poly (N-isopropylacrylamide). *Colloid Polym. Sci.* **2011**, *289* (15-16), 1777-1782.
- 33. Han, J.; Zheng, Y.; Zheng, S.; Li, S.; Hu, T.; Tang, A.; Gao, C., Water soluble octa-functionalized POSS: all-click chemistry synthesis and efficient host–guest encapsulation. *Chem. Commun.* **2014**, *50* (63), 8712-8714.
- 34. Lv, X.; Liu, C.; Song, S.; Qiao, Y.; Hu, Y.; Li, P.; Li, Z.; Sun, S., Construction of a quaternary ammonium salt platform with different alkyl groups for antibacterial and biosensor applications. *RSC Adv.* **2018**, *8* (6), 2941-2949.
- 35. Li, F.; Weir, M. D.; Xu, H. H. K., Effects of Quaternary Ammonium Chain Length on Antibacterial Bonding Agents. *J. Dent. Res.* **2013**, *92* (10), 932-938.
- 36. McDonnell, G.; Russell, A. D., Antiseptics and Disinfectants: Activity, Action, and Resistance. *Clin Microbiol. Rev.* **1999**, *12* (1), 147-179.
- 37. Salton, M., Lytic agents, cell permeability, and monolayer penetrability. *J. Gen. Physiol.* **1968,** *52* (1), 227-252.

- 38. Hellberg, P.-E.; Bergström, K.; Holmberg, K. Cleavable Surfactants. *J. Surfactants Deterg.* **3**, 2000, 81-91.
- 39. Wright, M. R. Arrhenius parameters for the acid hydrolysis of esters in aqueous solution. Part I. Glycine ethyl ester, β-alanine ethyl ester, acetylcholine, and methylbetaine methyl ester. *J. Chem. Soc.* B **1969**, 707-710
- 40. Thompson, R. A.; Allenmark, S. Factors influencing the micellar catalyzed hydrolysis of long-chain alkyl betainates. *J. Colloid Interf. Sci.* **1992**, 148, 241-246.
- 41. Bell, R. P.; Lindars, F. J. Kinetics of the acid and alkaline hydrolysis of ethoxycarbonylmethyltriethylammonium chloride. *J. Chem. Soc.* **1954**, 4601-4604
- 42. Liu, S. Q.; Yang, C.; Huang, Y.; Ding, X.; Li, Y.; Fan, W. M.; Hedrick, J. L.; Yang, Y. Y., Antimicrobial and antifouling hydrogels formed in situ from polycarbonate and poly (ethylene glycol) via Michael addition. *Adv. Mater.* **2012**, *24* (48), 6484-6489.
- 43. Zheng, J.; Li, L.; Tsao, H.-K.; Sheng, Y.-J.; Chen, S.; Jiang, S., Strong Repulsive Forces between Protein and Oligo (Ethylene Glycol) Self-Assembled Monolayers: A Molecular Simulation Study. *Biophys. J.* **2005**, *89* (1), 158-166.
- 44. Zheng, J.; Li, L.; Chen, S.; Jiang, S., Molecular Simulation Study of Water Interactions with Oligo (Ethylene Glycol)-Terminated Alkanethiol Self-Assembled Monolayers. *Langmuir* **2004**, *20* (20), 8931-8938.
- 45. Zhang, Z.; Chen, S.; Chang, Y.; Jiang, S., Surface grafted sulfobetaine polymers via atom transfer radical polymerization as superlow fouling coatings. *J. Phys. Chem. B* **2006**, *110* (22), 10799-10804.
- 46. Carr, L. R.; Zhou, Y.; Krause, J. E.; Xue, H.; Jiang, S., Uniform zwitterionic polymer hydrogels with a nonfouling and functionalizable crosslinker using photopolymerization. *Biomaterials* **2011**, *32* (29), 6893-6899.
- 47. Hellberg, P.-E.; Bergström, K.; Holmberg, K., Cleavable surfactants. *J. Surfactants Deterg.* **2000,** *3* (1), 81-91.

Table of Contents graphics (TOC)



Degradable and Antibacterial Hybrid Hydrogels with Robust Mechanical Properties